A computational two-photon fluorescence approach for revealing label-free the 3D image of viruses and bacteria

Cédric Delmon, Erwan Ferrandon, Emilie Chouzenoux, Audrey Prorot, Sophie Alain, Claire Lefort

A computational two-photon fluorescence approach for revealing label-free the 3D image of viruses and bacteria

Cédric Delmon[1], Erwan Ferrandon[2], Emilie Chouzenoux[3], Audrey Prorot[1], Sophie Alain[4], and Claire Lefort[2]*

[1]E2LIM, UR24133, University of Limoges, Limoges, France

[2]XLIM Research Institute, UMR CNRS 7252, University of Limoges, Limoges, France

[3]Center for Visual Computing, CentraleSupélec, Inria Saclay, Université Paris-Saclay, Gif-sur-Yvette, France

[4]RESINFIT, UMR INSERM 1092 University of Limoges, Bacteriology-Virology-Hygiene Department, University Hospital Center, France

***Claire Lefort, E-mail: claire.lefort@cnrs.fr

Abstract

Current solutions for bacteria and viruses identification are based on time-consuming technics with complex preparation procedures. In the present work, we revealed label-free the presence of free viral particles and bacteria with a computational two-photon fluorescence (C-TPF) strategy. Six bacteria were tested: *Escherichia coli*, *Staphylococcus epidermidis*, *Proteus vulgaris*, *Pseudomonas fluorescens*, *Bacillus subtilis* and *Clostridium perfringens*. The two families of viral particles were the herpes virus with the cytomegalovirus (CMV, 300 nm of diameter) and the coronavirus with the SARS-CoV-2 (100 nm of diameter). The instrumental and computational pipeline FAMOUS optimized the produced 3D images. The origin of the fluorescence emission was discussed for bacteria regarding to their two-photon excitation spectra and attributed to the metabolic indicators (FAD and NADH). The optical and computational strategy constitute a new approach for imaging label-free viral particles and bacteria and paves the way to a new understanding of viral or bacterial ways of infection.

Keywords: Two-photon fluorescence, bacteria, free-virions, SARS-CoV-2, metabolic indicators, computational restoration.

1 Introduction

Free viral particles – named virions – or bacteria constitute a set of biomedical objects of first interest in many medical or biological situations. Revealing their presence is a strategical concern for which several accurate solutions are routinely operated such as PCR (polymerase chain reaction),[1] conventional laboratory-based culture media, immunological techniques, flow cytometry, [2] or Raman spectroscopy.[3] A recent technical advance for detecting bacteria with fluorescence-based dyes has allowed to assess simultaneously their physiological states while targeting specific biomolecules and physiological processes.[3, 4] But these solutions do not deliver a result in live or *in situ* and are often expensive, time-consuming, associated with complex preparation procedures, or can lead to false positive/negative results. Two-photon fluorescence lifetime imaging (FLIM) delivers images of microbial systems at micrometric scale.[5, 6] However, the fluorescence decay is sensitive to physico-chemical properties of the containing medium such as pH, ionic composition (Na^+, K^+…) and temperature,[7] whereas basic two-photon fluorescence is not.

Optical solutions devoted to the imaging of microorganisms with dimensions competing with the diffraction limit is a challenge which has led to solutions of super-resolution microscopy.[8] While super-resolution strategies go beyond the diffraction limit, their technical use is complex and involves particularly sophisticated preparations from the laser system to the chemical substance for visualizing the object of interest. In that context, computational approaches associated with standard microscopy systems have gained a new interest while they are less complex from the instrumental view-point.[9-11, 6] However, restricting the observation of bacteria or virions to the 2D image of the focal plan of the microscope can induce false interpretations about the observed object. Indeed, the 2D visualization of a vertically oriented bacillus gives the appearance of a disk to the image, a pattern similar to that of a coccus observed in 2D. In that context, the 3D visualization becomes essential for the visual observation of these microorganisms.

In the present work, we have demonstrated the ability of a computational two-photon fluorescence strategy (C-TPF) to image label-free biomedical objects from different origin and presenting a dimension competing with the diffraction limit.[12, 13] First, six families of bacteria representing micrometric objects were imaged: *Bacillus subtilis* (*B. subtilis*), *Clostridium perfringens* (*C.*

perfringens), *Escherichia coli* (*E. coli*), *Pseudomonas fluorescens* (*P. fluorescens*), *Proteus vulgaris* (*P. vulgaris*), and *Staphylococcus epidermidis* (*S. epidermidis*). These six bacteria were chosen for their representative properties: Gram positive or negative, two shapes (bacilli or cocci), two kinds of respiratory metabolism (aerobic or anaerobic) and the sporulation ability. Then, smaller microorganisms were tested with two families of virions: the cytomegalovirus (CMV) the biggest specimen known from the family of herpes virus and the SARS-CoV-2, a small virion from the family of coronaviruses. To do so, the endogenous two-photon fluorescence signals were recorded and the resulting images were improved thanks to the pipeline FAMOUS.[14] Finally, the two-photon excitation spectra of bacteria were recorded and the origin of endogenous fluorescence and the related biosensors responsible from the nonlinear signal emitted were discussed.

2 Materiel and methods

2.1 Instrumental and computational strategy: the pipeline FAMOUS

The experimental system was based on a standard solution of multiphoton microscopy, associated with an original computational strategy of image restoration especially developed for the improvement of 3D multiphoton images. Figure 1 illustrates the experimental principle of the pipeline and the detailed protocol can be found in [14].

A commercial multiphoton microscope from Olympus (reference BX61WI) was involved for the whole setup and coupled with a mode-locked titanium-doped sapphire laser system (Ti: Sa) delivering femtosecond pulses in the near infrared range between 680 and 1080 nm (Chameleon Ultra II, Coherent). Two microscope objectives were used from Olympus: the XLPN-MP (25x, numerical aperture 1.05, water immersion, optical ICS: ∞, magnification 25, field number: 18) and the LUMPlanFL N (60x, numerical aperture 1.10, water immersion, optical ICS: ∞, magnification 63, field number: 26.5). The detection system was composed by two photomultipliers tubes (PMTs), each of them being coupled with a dichroic mirror (518 nm) and emission filters. The first PMT was associated with an emission filter detecting the range between 420 and 500 nm, the second one between 575 and 630 nm. The microscope objective was laser scanned with two galvanometric mirrors, thus supplying 2D images with a dimension of 512 × 512 pixels. The pixel

dwell-time was fixed at 2 µs/pixel producing a 2D image in 52 seconds. An axial shift of the microscope objective delivered 2D images all along the optical axis with a controlled spacing of 10 nm between two successive 2D images. By this method, 3D images were constructed from the superimposition of 2D images along the Z axis. About seventy 2D images had to be recorded along the Z axis for producing a 3D image available after thirty minutes of recording.

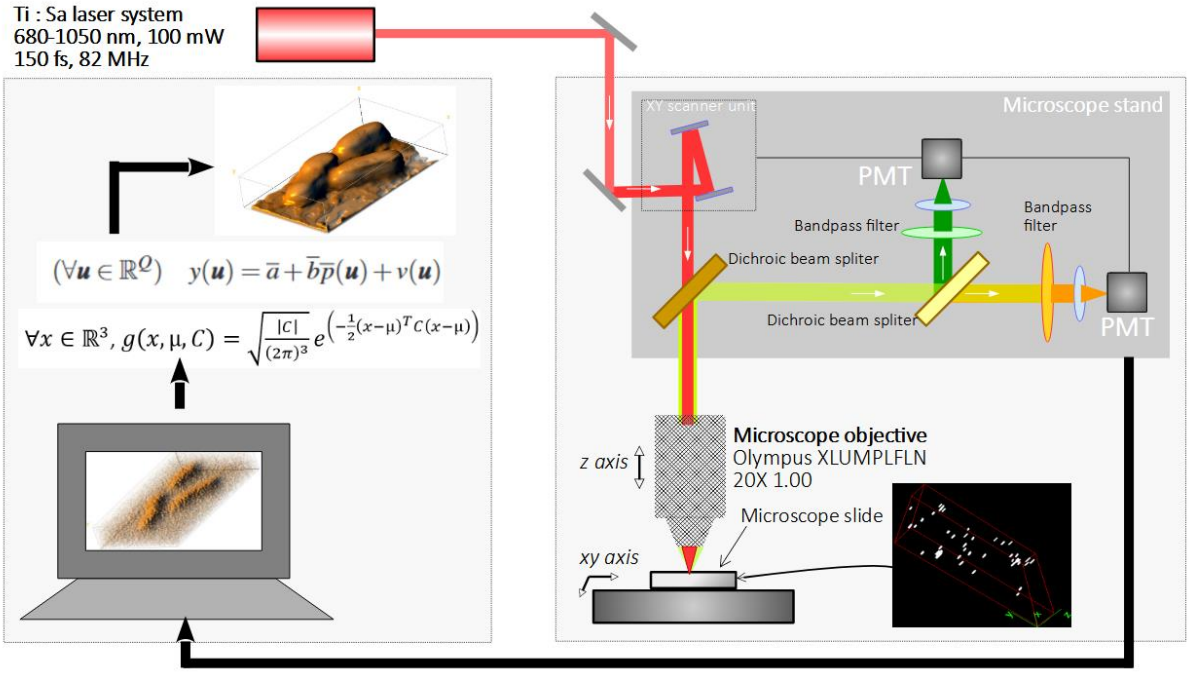

Figure 1. Experimental setup of C-TPF devoted to the image recording and reconstruction of bacteria and viruses.

The computational strategy followed a two-step approach. Figure 2 depicts the numerical process. In brief, the signal from the virions or bacteria was recorded simultaneously with the signal emitted from reference objects, here microspheres with a diameter smaller than the diffraction limit. This kind of micro-objects was a good candidate for the evaluation of the instrument response function named PSF for Point Spread Function. The PSF was then mathematically modeled with the FIGARO algorithm. This strategy fitted in situ the PSF with a multivariate gaussian function by relying on an advanced algorithmic approach we have demonstrated and detailed in.[15] Therefore the in situ estimation of the PSF took into consideration the optical distortions that can occur locally: variability of the concentration of scattering elements, local variations of refractive index.

Then, a procedure of image restoration was led with a deconvolution approach considering the learned PSF, combined with a denoising and deblurring method.

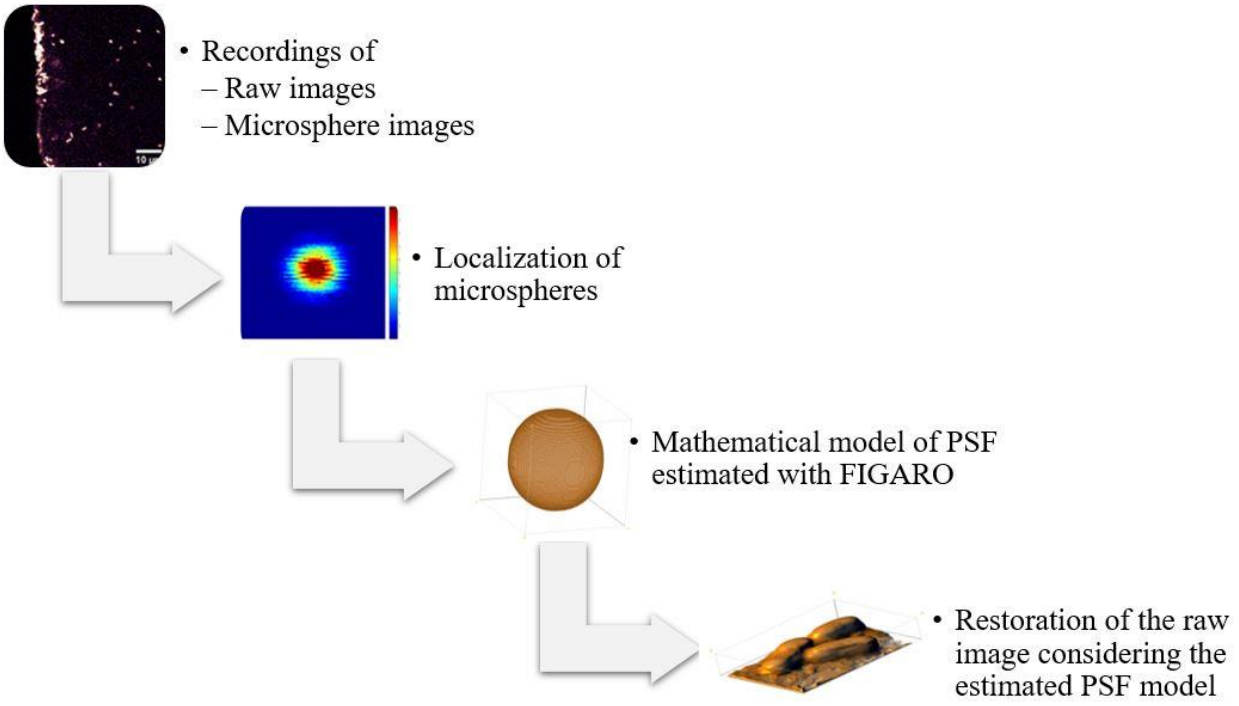

Figure 2. Computational pipeline for image restauration considering the PSF estimated in situ with a synchronized localization and recording with the biomedical object to restore.

2.2 Bacteria

2.2.1 Six bacteria

Bacteria are microorganisms classified in different categories. At first, Gram stain allows to distinguish Gram-positive and Gram-negative bacteria relatively to the more or less important presence of peptidoglycan into the bacterial wall. Then, a direct examination can discriminate two main bacteria shapes: bacilli (stick shape) or cocci (roundish shape). Moreover, other supplementary parameters can hone the categorization of bacteria: respiratory metabolism can be aerobic or anaerobic. Thus, aerobic bacteria need oxygen to grow whereas anaerobic bacteria grow without oxygen. Furthermore, some bacteria can resist to environmental stress by forming spore bacteria.

In that context, six different families of bacteria have been chosen in order to cover a maximum of bacterial categories. Table 1 gathers the main properties of the related bacteria covering a wide range of morphological features.[16]

Table 1. List of bacteria and their biological properties

	Gram	Shape	Aerobic	Anaerobic	Sporulation	Length (µm)	Diameter or width (µm)
B. subtilis	-	Bacillus	Strict		Yes	2 to 6	1
C. perfringens	+	Bacillus		Strict	Yes	3 to 8	0.4 to 1.2
E. coli	-	Bacillus	Yes	Facultative	No	1 to 2	1
P. fluorescens	-	Bacillus	Strict		No	2 to 2.5	0.5
P. vulgaris	-	Bacillus	Yes		No	1.2 to 2.5	0.4 to 0.6
S. epidermidis	+	Coccus	Yes	Facultative	No		0.5 to 1.5

The dimensions of the bacteria are in the range of the micrometer. For example, *B. subtilis* is 2-6 µm long with a diameter of 1 µm.[17] *C. perfringens* size is 3 to 8 µm long with a diameter between 0.4 and 1.2 µm. Concerning *E. coli*, these bacilli are 1-2 µm in length with 1 µm in width. *P. fluorescens* is longer than E. coli (2-2.5 µm long and 0.5 µm width). *P. vulgaris* sizes are contained between 1.2 to 2.5 µm long and 0.4 to 0.6 µm in diameter and *S. epidermidis* diameter is 0.5-1.5 µm.[18]

2.2.2 Protocol of preparation

Each bacteria were cultured in TSB culture medium (Trypto-Casein-Soy Broth BK046HA, Biokar®). To obtain optimal growth, bacteria were cultured for 2 to 3 days at 37°C. Then, 1.2 mL of different bacteria contained in TSB medium were centrifuged at room temperature for 15 minutes at 5400 rpm and the pellets were resuspended in 4mL of Phosphate Buffer Saline (PBS). Optical densities were measured at 600 nm ranging from 0.1 to 1.6. Samples were maintained at 4°C until microscopy analysis. To ensure that observed objects were actually microorganism, *E. coli* and *S. epidermidis* were stained with 5(6)-Carboxyfluorescein diacetate (CFDA). This label was selected to evaluate esterase activity. Thus, 1 mL of PBS containing microorganism was stained with CFDA (22 µM) and incubated during 30 minutes at 37°C. This solution was rinsed with PBS before observation.

2.3 Viruses

2.3.1 Two viruses tested

Two different kinds of free-virions were experienced for this study: CMV and SARS-CoV-2. The interest of CMV rests on its range of diameter from 150 to 200 nm, 300 nm for the biggest,[19] dimensions close to the diffraction limit of the microscopy system. Two strains of CMV were experimented: a fluorescent strain (BAD) once inside the cell and a label free one (VHLE). To validate that we were observing viral particles under the microscope, VHLE strain were marked by immunostaining. SARS-CoV-2, a well-known virus responsible for the pandemic situation, was the last biomedical object tested. Indeed, the diameter of SARS-CoV-2 virions is about 3 times smaller than the diffraction limit with a diameter between 60 and 140 nm.[20] By consequence, a detected signal can be expected from such objects without more information.

2.3.2 Protocol of preparation

Solutions containing viral particles from infected cell culture media were stored at -80°C. To eliminate cellular debris, the supernatant was clarified and then spent 30 seconds under UV to break the DNA/RNA bonds and to disable viral particles. The medium was then filtered by centrifugation in 4 mL Amicon tubes for 10 minutes at 5000 g. The filtrate was collected (200 µL) then transferred into 2 mL Eppendorf tubes and diluted by half in PBS. Magnetic beads on a magnetic rack filtered the viral particles: 40 µL of magnetic beads were added to the virion solution for an incubation of 10 minutes at room temperature and 30 minutes on a magnetic rack at room temperature. The viral particles coupled with magnetic beads were rinsed twice with PBS on a rack and then suspended in 100 µL of PBS.

VHLE viral particles were observed after fixation on beads and double immunostaining. The purpose of these marking is to find the viruses aggregates more easily under the microscope, have an idea of their shape/distribution on the slide and then compare the results without labelling. Viral particles coupled with magnetic particles were incubated in an oven at 37°C with anti-cytomegalovirus antibodies (Ab gB) diluted to 1/40th for 30 minutes without a magnetic rack and 30 minutes at room temperature on a magnetic rack, then washed three times in PBS. Then, the

viral particles were incubated away from light at 37°C with the anti-mouse antibodies, labeled with fluorescein, diluted to 1/100 th for 30 minutes without a magnetic rack and 30 minutes at 37°C on a magnetic rack and washed three times with PBS. Finally, the viral particles were resuspended in 100 µL of PBS. 10 µL from the solutions were placed between slide and coverslip in order to be observed under the microscope.

3 Results

3.1 Two-photon fluorescence observations of bacteria and virions label-free with C-TPF

From the instrumental point of view, bacteria and virions constitute a suitable set of microorganisms for evaluating the performance of such approach to visualize biomedical objects from different origins label-free and with a wide variety of dimensions. The instrumental and computational pipeline FAMOUS was used for revealing the presence of bacteria and virions in the sub-micrometer range and producing a 3D image of these objects. Figure 3 gathers the images of the six families of bacteria and the two families of virions recorded for the spectral range of emission between 420 and 500 nm. The second PMT, detecting the spectral range between 575 and 630 nm has recorded a very low signal difficult to exploit but colocalized with the detected objected with the first PMT. By evidence, the signals from each PMTs come from the same biological object.

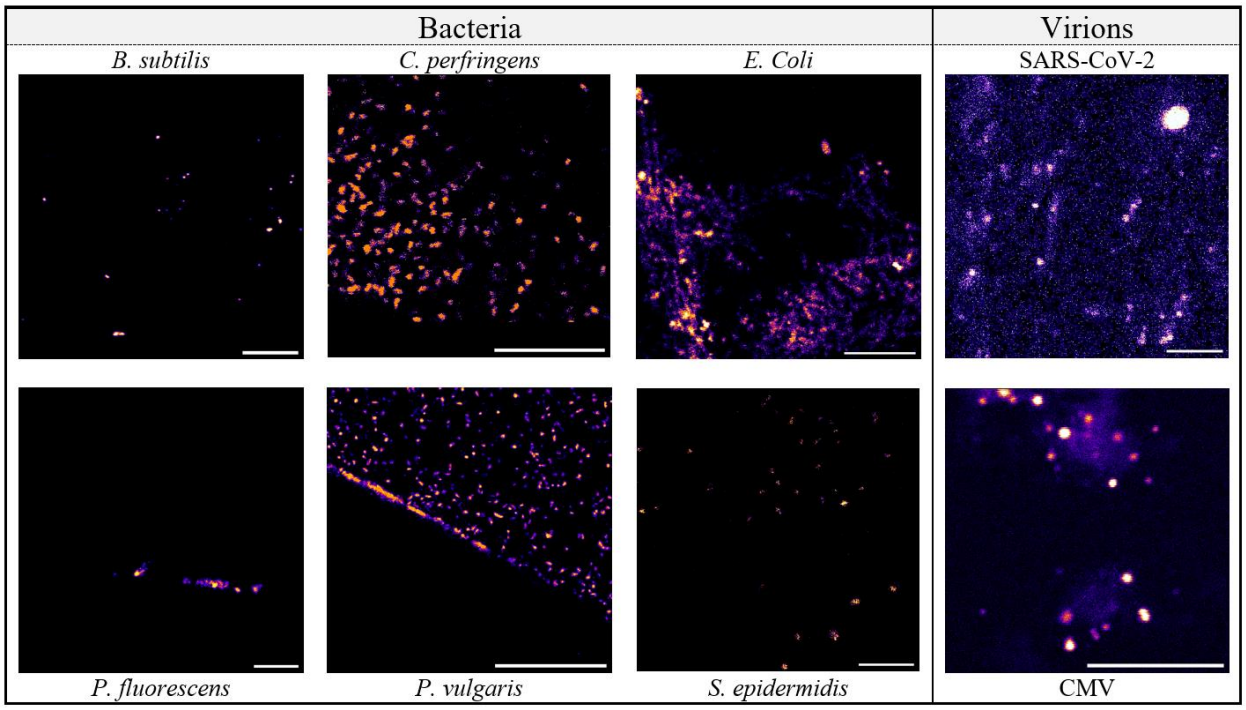

Figure 3. Raw two-photon fluorescence images of microorganisms recorded with an excitation wavelength fixed at 780 nm and a detection range between 420 and 500 nm. Scale bar: 10 µm. Viruses and bacteria had emitted a detectable signal label-free under the laser excitation.

The raw recordings presented into Figure 3 illustrate the fact that an optical solution of two-photon fluorescence is suitable to induce an endogenous fluorescence signal from these biomedical objects regardless of their origin: bacteria or virions. The organic origin of these microorganisms, constituted by complex assemblies of macromolecules with a high density of conjugated electrons, were favorable to the emission of an endogenous signal of fluorescence under a femtosecond laser excitation in the near infrared range. However, it is important to notice that the visual recognition of bacteria with the bacilli shapes (here five of the six families of bacteria, Table 1) was nearly impossible with the 2D images alone. Indeed, if the 2D image plan follows the bacterium's transversal axis, bacilli shapes are represented as spheroidal shapes. Reversely, if the 2D image follows the bacterium's longitudinal axis, bacilli shapes are represented as stick shape at the image. By evidence, the orientation of the main axis of bacteria is not a parameter that can be mastered in an environmental situation. By consequence, there is a specific need for a 3D representation of microorganisms.

3.2 3D representation of bacteria and virion

3D images of these biomedical objects were produced with an improved visual quality thanks to our instrumental and computational pipeline FAMOUS. Figure 4 illustrates the raw and reconstructed 3D observations of P. vulgaris and CMV. In supplementary file, a 3D movie allows the observation of P. vulgaris from all angle.

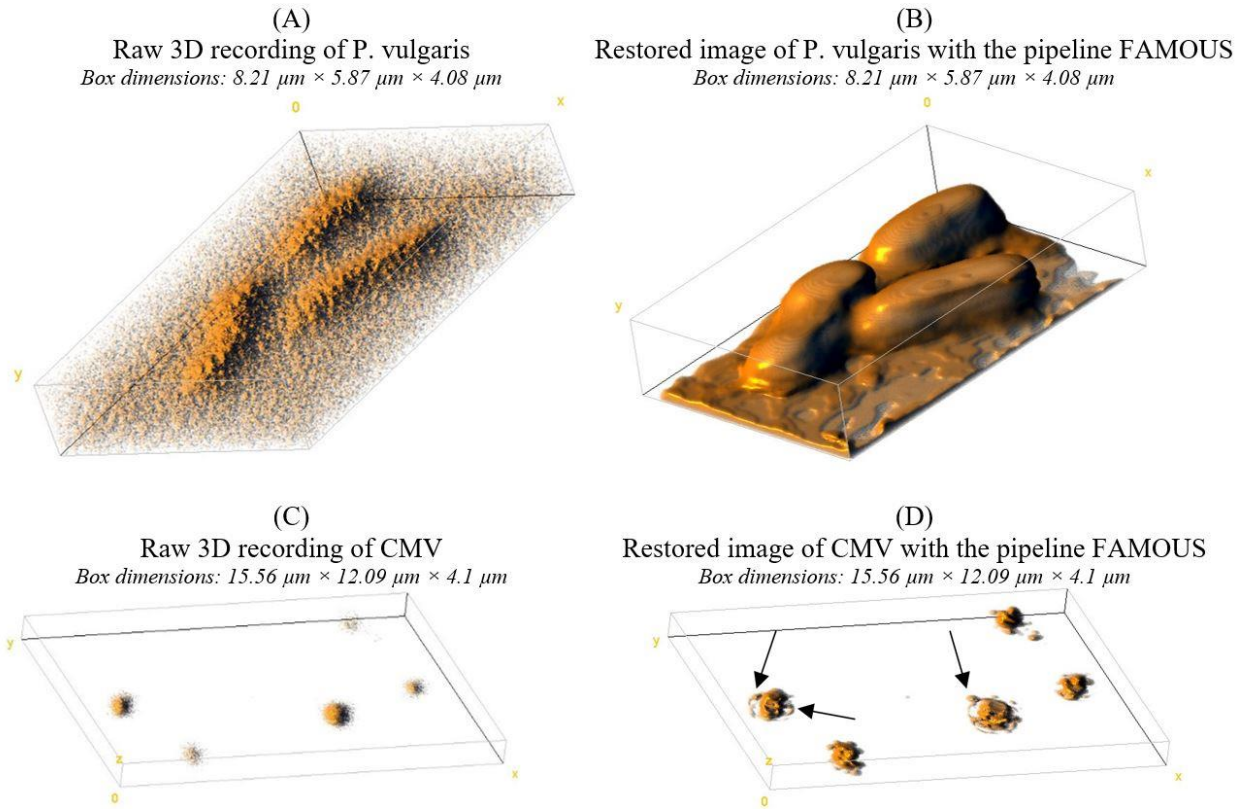

Figure 4. 3D observations of bacteria and virions thanks to the optical sectioning ability of multiphoton microscopy combined with our original instrumental and computational pipeline FAMOUS. A. Raw recording of *P. Vulgaris*. B. Resorted image of *P. Vulgaris*. C. Raw recording of CMV. D. Resorted image of CMV; the black arrows tip onto a halo that reminds individual particle into a bundle CMV. A supplementary file delivers a movie for the 3D restored image of *P. vulgaris*.

The improvement of the visual image quality was demonstrated in the present case for bacteria and virions. In the case of the virions of CMV, a halo of light coming from the smallest viral particles was detected and presented a diameter in the range of the diffraction limit. In both situations, the PSF estimation was led. The five-remaining families of bacteria have also been

observed in 3D. The produced image was similar between bacteria from the same shape family (Bacillus or Coccus) and their distinction was not possible for a human eye.

3.3 Characterization of two-photon fluorescence excitation spectra of bacteria

3.3.1. Two-photon fluorescence excitation spectra of bacteria

Each strain of bacteria was spectrally bench characterized. First, the emission range were estimated with a set of emission filters, highlighting an optimal emission range for the filter 420 and 500 nm for all of the bacteria. Then, the two-photon excitation spectra were measured for each bacteria by scanning the central wavelength of the Ti: Sa laser system between 680 and 1080 nm with a step of 20 nm. The laser average power was kept constant during the whole experiment. For each image, a ten of bacteria was selected and the related fluorescence intensity was measured as a function of the central wavelength of excitation. The emitted fluorescence intensities plotted as a function of the excitation average power were corresponding to the integration of the emitted intensity over the spectral range between 420 and 500 nm. Figure 5 presents the normalized two-photon excitation spectra of each bacteria.

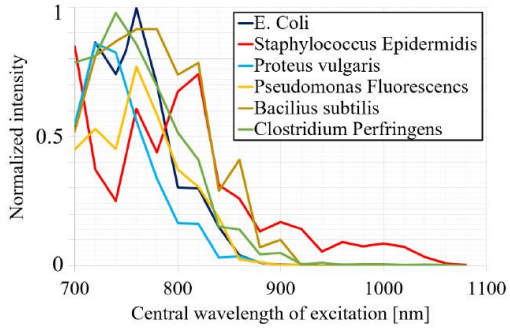

Figure 5. Two-photon excitation spectra recorded between 680 and 1080 nm with a step of 20 nm for each of the six bacteria.

We note here that the measurement of the two-photon fluorescence excitation spectra of virions was not possible due to the fragility of these microorganisms under a long exposure to the high peak power of the infrared laser radiations.

3.3.2. Characterization of two-photon processes in bacteria

The origin of endogenous fluorescence was investigated. First, the measurement of the order of the nonlinear process was led for three bacteria. Figure 6 highlights the logarithmic plot of the fluorescence intensities measured for *B. subtilis*, *P. fluorescens* and *P. vulgaris* depending on the logarithmic plot of the average power of the laser excitation between 30 mW, the smallest average power to observe bacteria, and 190 mW, the highest average power before the photo-destruction of the bacteria. The excitation wavelength was centered at 780 nm. The slopes respectively equal 2.152, 2.317 and 2.280 for *B. subtilis* (Figure 6A), *P. fluorescens* (Figure 6B) and *P. vulgaris* (Figure 6C). This kind of evolution illustrates a square dependence of fluorescence intensity resulting from a quadratic nonlinear process. This point is discussed in the following part.

(A)

B. subtilis

$I = 0{,}0303\ P^{2.152}$

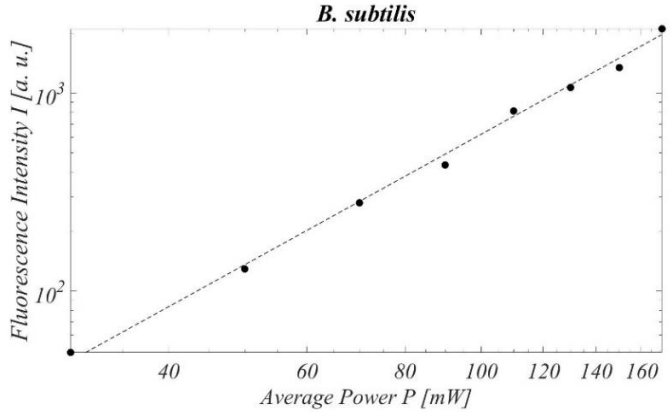

(B)

P. fluorescens

$I = 0{,}0132\ P^{2.317}$

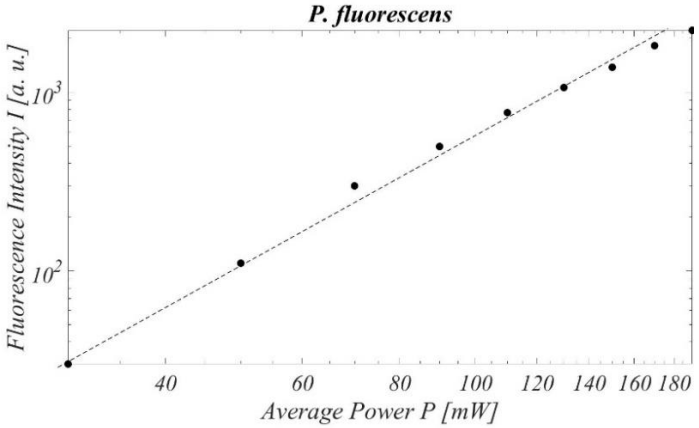

(C)

P. vulgaris

$I = 0{,}025\ P^{2.280}$

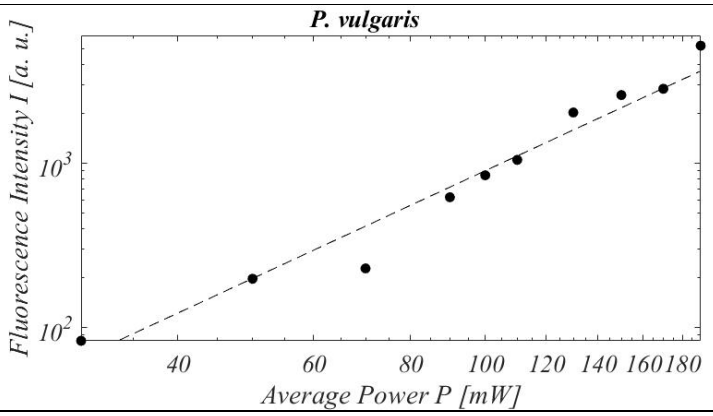

Figure 6. Fluorescence intensities of bacteria measured as a function of laser excitation average power for a central wavelength of 780 nm for (A) *B. subtilis*, (B) *P. fluorescens* and (C) *P. vulgaris*. The square dependence of fluorescence intensity results from a quadratic nonlinear process.

4 Discussion and perspectives

4.1 The interest of C-TPF and 3D representation of microorganisms

We have demonstrated that two-photon fluorescence is a nonlinear optical process able to produce detectable endogenous signals from bacteria and viral structures, irrespectively of their family. Therefore, the interest of C-TPF was established here for the first time to our knowledge as a solution able to produce images of bacteria and virions label-free. Such a technical solution is now ready to be included into the routine detection of bacteria. Moreover, the 3D image delivered by the C-TPF solution is essential for a visual recognition of these microorganism and for avoiding misinterpretation of the shapes observed on a 2D image. Finally, the 3D image is the exclusive solution able to deliver enough distinctive criteria to allow a computational strategy to distinguish and identify bacteria's family shape. These considerations pave the way to the implementation of a solution using artificial intelligence especially devoted to the identification of bacteria's family shape with an optical solution label-free.

4.2 Origin of the endogenous emission of fluorescence from bacteria

For all of the bacteria, the excitation range was below 900 nm. The six two-photon excitation ranges are contained between 700 and 850 nm at the full width at half maximum. Therefore, the spectral characterization of bacteria (Figure 5) has revealed a similar range of multiphoton excitation spectrum associated with a similar range of emission regardless of the bacteria's family. Moreover, the evolution of fluorescence intensity depending on average excitation power has revealed a non-strict two-photon process resulting from the complex biochemical composition. Thanks to this complex biochemical composition of bacteria and virions, two-photon fluorescence methods can highlight such microorganisms. At last, an optimization of this strategy and a preliminary accurate study of the quantity of detected microorganisms by C-TPF versus the real number of cells could allow to a useful microorganism's quantification method. Indeed, prokaryotic cells display an intrinsic natural fluorescence due to the presence of many fluorescent structural cellular components and metabolites. The emitted signal could originate from a part or a totality of these substances such as protein tryptophan, a few other aromatic amino acids, nucleic acids, and some coenzymes.[21-23] The emission spectra resulting from these substances emitting an endogenous signal of fluorescence cover most of these spectral ranges.[21] According to these authors, the influence of flavin adenine dinucleotide (FAD) and nicotinamide-adenine dinucleotide (NAD) are considered to be major. Because of its key role in the conversion of energy, the fluorescence of reduced nicotinamide-adenine dinucleotide (NADH) and oxidized FAD can be used as metabolic biomarker of cell. Moreover, various optical studies described in the literature present the two-photon excitation and emission spectra of fluorescence of NADH and FAD and three-photon excitation of tryptophan or nucleic acids.[23-28] All of these studies display a two-photon excitation range of NADH and FAD located between 700 and 850 nm – as we have measured – and an emission range, centered at 450 nm covering the range between 400 and 600 nm. This spectral range corresponds to the emission range we have detected. Considering that all alive bacteria contain metabolic indicators, this cluster of clues leads us to suppose that the fluorescence emission detected from bacteria in this study arises from these metabolic components instead of structural membrane proteins. Therefore, the emission of fluorescence should be detected for all the bacteria with metabolic activity. Further investigations are needed to confirm this hypothesis and paves the way to a new solution for the quantification of bacteria.

5 Conclusion

Computational two-photon fluorescence (C-TPF) has been used for revealing label-free the presence of free viral particles named virions and bacteria. The six populations of bacteria and the two populations of virions tested were processed by the instrumental and computational pipeline FAMOUS delivering label-free images visually optimized of these objects. Regarding to the two-photon excitation spectra characterized from the six families of bacteria, the origin of the detected fluorescence signal was attributed to the metabolic indicators: flavin adenine dinucleotide (FAD) and nicotinamide-adenine dinucleotide (NADH). Through our results, we have demonstrated a new approach with the association between an optical solution and a computational strategy adapted for revealing label-free the presence of virus and bacteria. A visual information could now be implemented thanks to this new approach which could play a new role for the understanding of viral or bacterial ways of infection.

Acknowledgments

This research was conducted as the part covering the “sciences and technics” and “health sciences” parts of the interdisciplinary research program CoviZion “Storytelling of a Virus: Representations, Images and Imaginations. Represent and Understand in Order to Act Better and Live with it”, funded by AMI FLASH Research and Innovations COVID of Nouvelle-Aquitaine, France.
We especially thanks Pr Jean-Christophe Pesquet for his enlightened opinion about this work and Pr Christophe Dagot for the first set of experiments of multiphoton imaging with bacteria. We especially thanks the GDR Imabio from CNRS for his financial support for Erwan Ferrandon.

Conflict of Interest

The authors declare no financial or commercial conflict of interest.

References

[1] U. Reischl, M. T. Youssef, J. Kilwinski, J. Kilwinski, N. A. Strockbine, “Real-time fluorescence PCR assays for detection and characterization of Shiga toxin, intimin, and enterohemolysin genes from Shiga toxin-producing Escherichia coli”, Journal of Clinical Microbiology, 40(7), 2555-65 (2002)

[2] E. Prest, F. Hammes, S. Kötzsch, M. C. M. van Loosdrecht, J. S. Vrouwenvelder, “Monitoring microbiological changes in drinking water systems using a fast and reproducible flow cytometric method”, Water Res, 47(19), 7131-42 (2013)

[3] S. A. Yoon, S. Y. Park, Y. Cha, L. Gopala, M. H. Lee, “Strategies of Detecting Bacteria Using Fluorescence-Based Dyes”, Frontiers in chemistry, 9, 743923 (2021)

[4] M. G. Wilkinson, “Flow cytometry as a potential method of measuring bacterial viability in probiotic products”, Trends in Food Science and Technology, 78, 1-10 (2018)

[5] N. Sapermsap, D. Day-Uei Li, R. Al-Hemedawi, Y. Li, J. Yu, D. JS Birch, Y. Chen, “A rapid analysis platform for investigating the cellular locations of bacteria using two-photon fluorescence lifetime imaging microscopy”, Methods and Applications in Fluorescence, 8 034001 (2020)

[6] J. Lee, R. Hestrin, E. E. Nuccio, K. D. Morrison, C. E. Ramon, T. J. Samo, J. Pett-Ridge, S. S. Ly, T. A. Laurence, P. K. Weber, “Label-Free Multiphoton Imaging of Microbes in Root, Mineral, and Soil Matrices with Time-Gated Coherent Raman and Fluorescence Lifetime Imaging”, Environmental Science and Technology, 56 (3), 1994-2008 (2022)

[7] L. Marcu, P. M. W. French, D. S. Elso, “Fluorescence Lifetime Spectroscopy and Imaging: Principles and Applications in Biomedical Diagnostics”, CRC Press 1 – 536 (2014)

[8] G. Huszka, M. A. M. Gijs, “Super-resolution optical imaging: A comparison”, Micro and Nano Engineering, 2, 7 – 28 (2019)

[9] G. Vicidomini, P. Boccacci, A. Diaspro, M. Bertero, “Application of the split-gradient method to 3D image deconvolution in fluorescence microscopy”, Journal of Microscopy, 234 (1), 47 – 61 (2009)

[10] E. Cueva, M. Courdurier, A. Osses, V. Castañeda, B. Palacios, S. Härtel, “Mathematical modeling for 2D light-sheet fluorescence microscopy image reconstruction”, Inverse Problems, 36 075005 (2020)

[11] E. J. Reid, L. F. Drummy, C. A. Bouman, G. T. Buzzard, “Multi-Resolution Data Fusion for Super Resolution Imaging”, IEEE Transactions on Computational Imaging, 8, 81-95 (2021)

[12] A. Diaspro, P. Bianchini, G. Vicidomini, M. Faretta, P. Ramoino, C. Usai, “Multi-photon excitation microscopy”, BioMedical Engineering OnLine, 5, 36 (2006)

[13] A. M. Larson, “Multiphoton microscopy”, Nat. Photonics, 5, 1 (2011)

[14] C. Lefort, M. Chalvidal, A. Paretné, V. Blanquet, H. Massias, L. Magnol, E. Chouzenoux, “FAMOUS: a fast instrumental and computational pipeline for multiphoton microscopy applied to 3D imaging of muscle ultrastructure”, J. Phys. D: Appl. Phys. 54, 274005 (2021)

[15] E. Chouzenoux, T.T.K. Lau, C. Lefort, J.-C. Pesquet, “Optimal multivariate Gaussian fitting with applications to PSF modeling in two-photon microscopy imaging”, J. Math. Imaging Vis., 61 1037–50 (2019)

[16] L. M. Prescott, J. M. Willey, L. M. Sherwood, C. J. Woolverton, J. Coyette, J.-P. Joseleau, R. Perraud, “Prescott's Microbiology”, 5th edition, De Boeck supérieur (2018)

[17] J. Errington, L. T van der Aart, “Microbe Profile: Bacillus subtilis: model organism for cellular development, and industrial workhorse”, Microbiology (Reading), 166 (5), 425–427 (2020).

[18] National Research Council (US) Steering Group for the Workshop on Size Limits of Very Small Microorganisms. Size Limits of Very Small Microorganisms: Proceedings of a Workshop. Washington (DC): National Academies Press (1999)

[19] V. Schottstedt, J. Blümel, R. Burger, C. Drosten, A. Gröner, L. Gürtler, M. Heiden, M. Hildebrandt, B. Jansen, T. Montag-Lessing, R. Offergeld, G. Pauli, R. Seitz, U. Schlenkrich, J. Strobel, H. Willkommen, C. H. von König, “Human Cytomegalovirus (HCMV)”, Transfusion medicine and hemotherapy, 37(6), 365–375 (2010)

[20] Y. M. Bar-On, A. Flamholz, R. Phillips, R. Milo, “SARS-CoV-2 (COVID-19) by the numbers”. eLife, 9, e57309 (2020)

[21] J. Surre, C. Saint-Ruf, V. Collin, S. Orenga, “Strong increase in the autofluorescence of cells signals struggle for survival”, Scientific reports (8) 12088 (2018)

[22] K. Torno, B. K. Wright, M. J. Jones, M. A. Digman, E. Gratton, M. Phillips, “Real-time analysis of metabolic activity within Lactobacillus acidophilus by phasor Fluorescence Lifetime Imaging Microscopy of NADH”, Curr Microbiol, 66, 365–367 (2013)

[23] T. Hortholary, C. Carrion, E. Chouzenoux, J.-C. Pesquet, C. Lefort, “Multiplex-multiphoton microscopy and computational strategy for biomedical imaging”, Microscopy Research and Technics 84 (7), 1553-1562 (2021)

[24] Y. Qin, Y. Xia, “Simultaneous Two-Photon Fluorescence Microscopy of NADH and FAD Using Pixel-to-Pixel Wavelength-Switching”, Frontiers in Physics, 9, 642302 (2021)

[25] I. Georgakoudi, K. P. Quinn, “Optical imaging using endogenous contrast to assess metabolic state”, Annual Review of Biomedical Engineering ,14, 351-367 (2012)

[26] J. R. Lakowicz, “Principles of Fluorescence Spectroscopy”, Springer, Third Edition (2006)

[27] E. Katilius, N. W. Woodbury, “Multiphoton excitation of fluorescent DNA base analogs”, Journal of Biomedical Optics, 11 (4), 044004 (2006)

[28] D. Nobis, R. S. Fisher, M. Simmermacher, P. A. Hopkins, Y. Tor, A. C. Jones, S. W. Magennis, “Single-Molecule Detection of a Fluorescent Nucleobase Analogue via Multiphoton Excitation”, Journal of Physical Chemistry Letters, 10 (17), 5008 - 50125 (2019)